PROCEEDINGS of the
23rd International Congress on Acoustics
9 to 13 September 2019 in Aachen, Germany

Practical Consideration and Implementation for Avoiding Saturation of Large Amplitude Active Noise Control

Dongyuan Shi[(1)], Woon-Seng Gan[(2)], Bhan Lam[(3)], Shulin Wen[(4)]

[(1-4)]School of Electrical and Electronic Engineering, Nanyang Technological University, Singapore
[(1-4)]DSHI003@e.ntu.edu.sg, EWSGAN@ntu.edu.sg, bhanlam@ntu.edu.sg, alicia.wen@ntu.edu.sg

Abstract

The saturation distortion of the power amplifier is a common and intractable issue for most audio devices, let alone for the active noise control (ANC) system. The effect of amplitude and phase distortion, caused by the saturated audio amplifier, on the adaptive algorithm in ANC is elaborated in this paper. To overcome this issue, the previously proposed the two-gradient FxLMS algorithm is applied, which efficiently suppresses the amplifier saturation and has as the same computational complexity as the FxLMS algorithm. The performance of the 2GD-FxLMS algorithm is experimentally validated for the first time in the control of both periodic and broadband signals.

Keywords: Saturation distortion, 2GD-FxLMS, Output constraint, Active noise control.

1 INTRODUCTION

Active noise control (ANC), which generates anti-noise waves that destructively interfere with the unwanted noise [1], is widely deployed in headphones [2], and other areas [3–9]. Similar to other audio devices, over-driving the audio amplifier to saturation usually results in degradation in active noise reduction performance and sound quality. Moreover, the amplitude and phase distortions caused by the saturated amplifier often result in the divergence of the adaptive algorithm.

Saturation distortion often happens when the output signal exceeds the output-power limits and hence, overdrives the amplifier [10]. Be specific. Saturation distortion is usually composed of the amplitude and phase distortion, which play the central role in the nonlinear property of the secondary path in ANC. Accordingly, the nonlinear adaptive algorithm seems to be an effective solution in overcoming the saturation distortion incurred in the ANC system [11]. In general, when the power amplifiers are partially overdriven, the typical nonlinear algorithm either using a truncated Volterra series [12] or a functional link artificial neural network (FLANN) [13, 14] can improve the noise reduction performance and convergence speed. However, the enormous computational expense of the nonlinear ANC algorithms always undermines their practicality. More importantly, when the magnitude of the optimal control signal (desired control signal) largely exceeds the threshold of the amplifier, neither the linear nor nonlinear ANC algorithms provide sufficient power to cancel the disturbance [10, 15]. The residual disturbance signal continuously accumulates in the control filter's coefficients and may result in overflow. Therefore, the nonlinear adaptive algorithm may not be the best solution for the saturation distortion in ANC when the amplifier is severely overdriven [16].

An alternative approach is to confine the output power of the audio amplifier to prevent it from being overdriven, and to maintain a specified power budget [17–19]. For instance, the clipping algorithm can truncate the part of the output signal above the limitation of the amplifier but at the expense of its stability and convergence speed [16]. Some of the latest clipping algorithms, which include the improved method, the rescale algorithm, using the projection method, which not only restricts the overdriven signal within the output constraint, but also rescales the weight of control filter to stabilize the algorithm [16, 20]. The leaky-type FxLMS algorithm introduces a leakage or penalization factor in the cost function to constrain the control effort and stabilize the adaptation [21]. However, these algorithms do not impose a specified constraint and only adjusts the leakage factor by trial and error to meet the power budget requirement. Therefore, a two-gradient FxLMS (2GD-FxLMS)

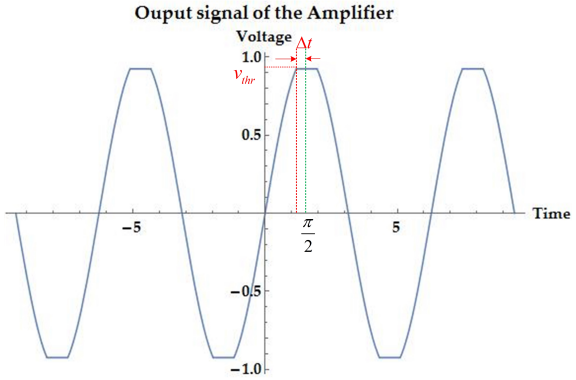

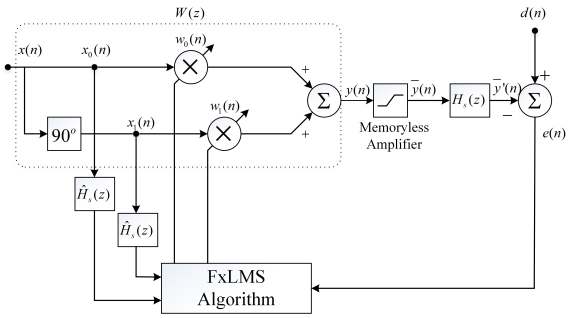

Figure 1. A periodic signal with amplitude distortion. Figure 2. A periodic signal with amplitude distortion.

algorithm, which imposes a specified output constraint with the same computational complexity as conventional FxLMS, was recently proposed [22]. It uses the Hemstitching method [23] to switch the gradient direction of the FxLMS algorithm to avoid the saturation distortion when the output signal violates the constraint and finally converges to the optimal control solution within the output constraint. Hence, this paper seeks to experimentally validate the previously proposed 2GD-FXLMS algorithm.

2 PROBLEM FORMULATION

This practical implementation is targeted at the audio amplifier, which is natively restricted by its electrical properties, especially its maximum output power. If the output signal exceeds its maximum allowance, the amplifier becomes saturated, resulting in amplitude and phase distortion, deteriorating the noise reduction performance and stability of ANC.

2.1 Amplitude distortion

Amplitude distortion arises when the part of the signal, whose amplitude is above the threshold (the maximum output amplitude of the amplifier), is clipped. For instance, we consider an audio amplifier with unity gain and the amplifier threshold of V_{thr}. If an input signal $x(t) = A\sin(\omega_0 t)$ has an amplitude of A larger than V_{thr}, the amplifier's output signal is clipped to

$$y(t) = \begin{cases} V_{\text{thr}}, & \omega_0 t + 2k\pi \in [\frac{\pi}{2} - \Delta t, \frac{\pi}{2} + \Delta t] \\ A\sin(\omega_0 t), & \text{otherwise} \\ -V_{\text{thr}}, & \omega_0 t + 2k\pi \in [\frac{3\pi}{2} - \Delta t, \frac{3\pi}{2} + \Delta t] \end{cases} \tag{1}$$

as shown in Fig. 1, where $\Delta t = \frac{\pi}{2} - \arcsin(V_{\text{thr}}/A)$ and $k \in \mathbb{Z}$. Its Fourier series can be rewritten as

$$y(t) = \frac{-2\Delta t + \pi + \sin(2\Delta t)}{\pi} A\sin(\omega_0 t) + \frac{4\cos(\Delta t)\sin^3(\Delta t)}{3\pi} A\sin(3\omega_0 t) + \ldots \tag{2}$$

It is clear that harmonic components are generated as a result of amplitude distortion. Figure. 2 illustrates a single-frequency adaptive noise canceller with a saturated amplifier model whose amplitude threshold is V_{thr}. The secondary path transfer function denoted by $H_s(z)$ has a gain of A_s. The noise disturbance $d(n) = D\sin(\omega_0 n)$ has an amplitude of D at the single frequency ω_0. The reference signal $x(n) = \sin(\omega_0 n + \theta_r)$ is of the same frequency but at a different initial phase θ_r as the disturbance. As the amplitude of the disturbance decides the status of the audio amplifier [10], there is no distortion when the amplitude is $D \in [0, A_s V_{\text{thr}}]$. When

$D \in (A_s V_{thr}, \frac{4A_s V_{thr}}{\pi}]$, the amplifier is moderately overdriven, and the disturbance can be entirely canceled at the fundamental harmonic, but some harmonics are also generated. Once the amplitude becomes $D \in (\frac{4A_s V_{thr}}{\pi}, \infty)$, the disturbance is only partially suppressed. The residual signals will drive the control filter coefficients unboundedly until it overflows.

2.2 Phase distortion

In many applications, the saturation of the amplifier often results in phase distortion, which in turns contributes to additional phase shift (phase error) in the secondary path. The disturbance is rewritten as its Fourier series [24]

$$d(n) = \sum_{k=-\infty}^{\infty} \overline{D}_k = \sum_{k=-\infty}^{\infty} D_k e^{jk\omega_0 n} \tag{3}$$

where D_k represents the amplitude of the kth harmonic. The output signal of the control filter is given by

$$y(n) = \sum_{k=-\infty}^{\infty} \overline{Y}_k = \sum_{k=-\infty}^{\infty} Y_k e^{jk\omega_0 n}. \tag{4}$$

Hence, the square error of the noise canceller is stated to

$$J = \mathbb{E}\left\{ \sum_{k=-\infty}^{\infty} \|E_k\|^2 \right\} = \mathbb{E}\left\{ \sum_{\mathbf{k}=-\infty}^{\infty} \left\| \overline{D}_k - H_s\left(e^{jk\omega_0}\right) \overline{Y}_k \right\|^2 \right\} \tag{5}$$

where $\mathbb{E}\{\cdot\}$ denotes the expectation operation. According to the least mean square (LMS) error method, the new output is derived as

$$\overline{Y}_k(n+1) = \overline{Y}_k(n) + \mu H_s^*\left(e^{jk\omega_0}\right) E_k(n) \tag{6}$$

where μ is the step size. When the amplifier enters the saturation, a phase error θ_a is brought into the secondary path. So, (6) is rewritten as

$$\overline{Y}_k(n+1) = \overline{Y}_k(n) + \mu H_s^*\left(e^{jk\omega_0}\right) e^{j\theta_a} E_k(n). \tag{7}$$

Substituting the optimal solution Y_k^o into (7) yields

$$\overline{Y}_k(n+1) - \overline{Y}_k^o = \left[1 - \mu e^{j\theta_a} H_s^*\left(e^{jk\omega_0}\right) H_s\left(e^{jk\omega_0}\right)\right] \left[\overline{Y}_k(n) - \overline{Y}_k^o\right]. \tag{8}$$

Hence, to guarantee the convergence of (7), the phase error should be

$$|\theta_a| < \arccos\left[\frac{\mu}{2} H_s^*\left(e^{jk\omega_0}\right) H_s\left(e^{jk\omega_0}\right)\right]. \tag{9}$$

If the phase error, caused by the amplifier's saturation, exceeds this bound, it may deteriorate the system's stability.

3 TWO-GRADIENT FILTERED-X LEAST MEAN SQUARES (2GD-FXLMS) ALGORITHM

To confine the output power of the amplifier while maximumly reducing the disturbance, we define a new cost function for the active control problem as

$$\begin{aligned} &\min_{\mathbf{w}} J(\mathbf{w}) = \mathbb{E}\left[\left| d(n) - \sum_{l=0}^{L-1} s_l \mathbf{w}^T(n-l)\mathbf{x}(n-l) \right|^2 \right] \\ &\text{s.t. } g(\mathbf{w}) = \mathbb{E}\left[\left| \mathbf{w}^T(n)\mathbf{x}(n) \right|^2 \right] \le \rho^2 \end{aligned} \tag{10}$$

Table 1. Pseudocode of 2GD-FxLMS algorithm

Two gradients FxLMS algorithm (2GD-FxLMS)
Input: Reference signal $x(n)$ and error signal $e(n)$.
Output: Clipped output signal $y_{\text{out}}(n)$.
Step 1: $y(n) = \mathbf{w}^{\mathrm{T}}(n)\mathbf{x}(n)$;
$x'(n) = \hat{\mathbf{s}}^{\mathrm{T}}(n)\mathbf{x}(n)$.
Step 2: If $\lvert y(n)\rvert \le \rho$
$\mathbf{w}(n+1) = \mathbf{w}(n) + \mu_1 e(n)\mathbf{x}'(n)$;
else
$\mathbf{w}(n+1) = \mathbf{w}(n) - \mu_2 y(n)\mathbf{x}(n)$.
Step 3: If $y(n) > \rho, \quad y_{\text{out}}(n) = \rho$
else if $y(n) < -\rho, \quad y_{\text{out}}(n) = -\rho$
else $y_{\text{out}}(n) = y(n)$.

where $|\cdot|$ denotes the absolute value. s_{l} is the lth coefficient of the secondary path $H_{\text{s}}(z)$ of length L, and $\mathbf{x}(n)$ and $\mathbf{w}(n)$ represent the reference signal and the control filter's weight vector, respectively. ρ^2 is the constraint on the power of the output signal. According to the Kuhn-Tucker condition [25], the (10) has only one optimal solution as

$$\mathbf{w}_{\text{o}} = (\lambda_{\text{o}}\mathbf{R}_{\text{xx}} + \mathbf{R}_{\text{x}'\text{x}'})^{-1}\mathbf{P}_{\text{dx}'} \tag{11}$$

where $\mathbf{R}_{\text{xx}}$ and $\mathbf{R}_{\text{x}'\text{x}'}$ represent the autocorrelation matrix of the reference $x(n)$ and filtered reference

$$x'(n) = \sum_{\text{l}=0}^{\text{L}-1} s_{\text{l}} x(n-l) \tag{12}$$

and $\mathbf{P}_{\text{dx}'}$ denotes the cross-correlation vector of $\mathbb{E}[d(n)\mathbf{x}'(n)]$. λ_{o} is the Lagrangian factor given by

$$\lambda_{\text{o}} = \frac{\mathbb{E}\{y'_{\text{o}}(n)[d(n) - y'_{\text{o}}(n)]\}}{\rho^2} \ge 0, \tag{13}$$

where the optimal anti-noise is

$$y'_{\text{o}}(n) = \sum_{\text{l}=0}^{\text{L}-1} s_l \mathbf{w}_{\text{o}}^{\mathrm{T}}\mathbf{x}(n-l). \tag{14}$$

To achieve the optimal solution of (10), we utilize the hemstitching method to derive the recursive formula of the control filter. When the output power of the control is within the constraint ($\mathbb{E}[y(n)^2] = \mathbb{E}\left[\left|\mathbf{w}^{\mathrm{T}}(n)\mathbf{x}(n)\right|^2\right] \le \rho^2$), the weight update is given by

$$\mathbf{w}(n+1) = \mathbf{w}(n) - \frac{1}{2}\mu_1 \frac{\nabla J(\mathbf{w})}{||\nabla J(\mathbf{w})||}. \tag{15}$$

In contrast, when the output power exceeds the constraint ($\mathbb{E}\left[\left|\mathbf{w}^{\mathrm{T}}(n)\mathbf{x}(n)\right|^2\right] > \rho^2$), the weight update changes to

$$\mathbf{w}(n+1) = \mathbf{w}(n) - \frac{1}{2}\mu_2 \frac{\nabla g(\mathbf{w})}{||\nabla g(\mathbf{w})||} \tag{16}$$

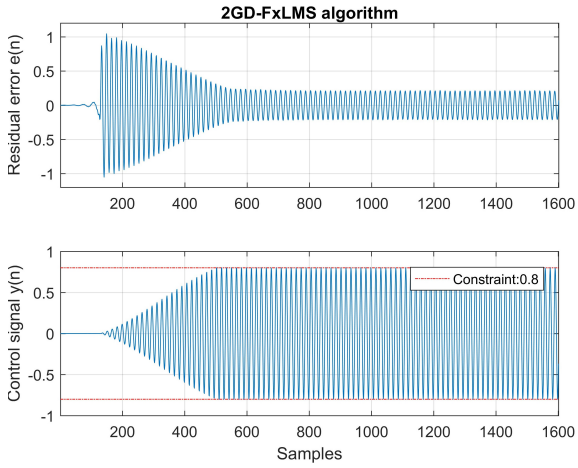

Figure 3. The error signal (top) and control signal (bottom) of the 2GD-FxLMS algorithm with an out- put constraint of 0.8.

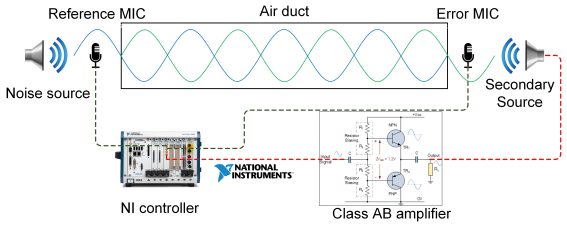

Figure 4. The active noise control air duct with the Class-AB (TDA2030A) audio amplifier.

where $||\cdot||$ denotes the Euclidean distance, and μ_1 and μ_2 are the step sizes. To further reduce the computation, we approximated the gradient in (15) and (16) by their instantaneous values as

$$\begin{cases} \nabla J(\mathbf{w}) &= -2e(n)\mathbf{x}'(n) \\ \nabla g(\mathbf{w}) &= \quad 2y(n)\mathbf{x}(n). \end{cases} \tag{17}$$

By substituting (17) into (15) and (16), and replacing the normalized gradient and average power constraint with the instantaneous gradient and amplitude constraint, the update equation is expressed as

$$\mathbf{w}(n+1) = \mathbf{w}(n) + \mu_1 e(n)\mathbf{x}'(n) \tag{18}$$

when the output signal $|y(n)| = |\mathbf{w}^{\mathrm{T}}(n)\mathbf{x}(n)| \leq \rho$, while

$$\mathbf{w}(n+1) = \mathbf{w}(n) - \mu_2 y(n)\mathbf{x}(n) \tag{19}$$

when $|y(n)| > \rho$. To guarantee that the output signal falls within the constraint, the output signal is clipped

$$y_{\mathrm{out}}(n) = \begin{cases} \rho & y(n) > \rho \\ -\rho & y(n) < -\rho \\ y(n) & \text{others.} \end{cases} \tag{20}$$

From (18) and (19), the algorithm operates with two different gradients, giving rise to its name: two gradients FxLMS (2GD-FxLMS). The 2GD-FxLMS uses the first term of (17) (as the same as conventional FxLMS) in updating the control filter to cancel the disturbance, when the output signal is within the output constraint. However, when the output violates the constraint, the algorithm adopts the second term of (17) to minimize the power of the output signal.

4 IMPLEMENTATION OF ALGORITHM

To use the 2GD-FxLMS algorithm for avoiding amplifier saturation, the following procedure is implemented.

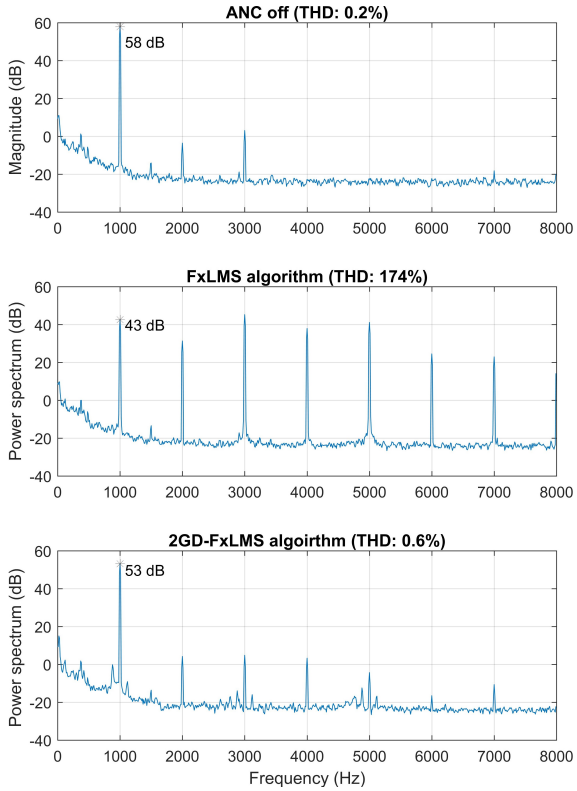

Figure 5. Error signals' power spectrum of FxLMS and 2GD-FxLMS for the tonal noise.

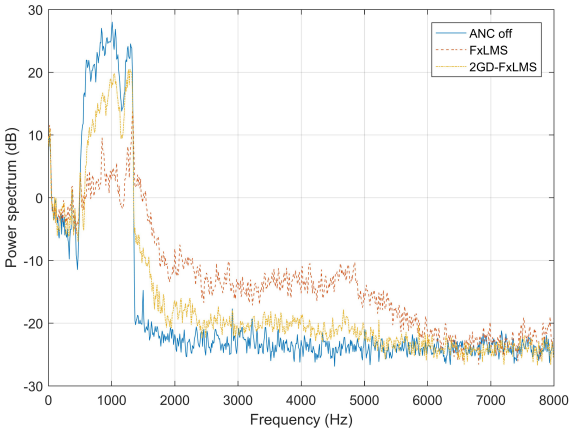

Figure 6. Error signals' power spectrum of FxLMS and 2GD-FxLMS for the broadband noise.

Stage 1: Obtain the threshold ρ^2 of the power amplifier by experimental measurement or referring to its manual book.

Stage 2: Implement 2GD-FxLMS as described in Table 1. It is noted that a 2GD-FxLMS, which consists of the control filter with M taps and the secondary path estimate with L taps, requires $2M+L+1$ multiplications and $2M+L-2$ additions, which is the same as the conventional FxLMS.

Stage 3: Determine μ_1 as the conventional FxLMS. Facing severe saturation distortion, adopt a large μ_2 to exert a tight restraint on the output power. However, if higher noise reduction with slight distortion is acceptable, a small μ_2 is more suitable.

5 SIMULATION RESULTS

In the simulation, the primary and secondary paths were measured from an air duct. The sampling rate and primary noise's frequency were set to 16 kHz and 1 kHz, respectively. The step size μ_1 and μ_2 in 2GD-FxLMS were both chosen as 5×10^{-5}, and the output constraint was set 0.8. Fig. 3 validates that 2GD-FxLMS can confine the output signal within the constraint while reducing the disturbance to a certain extent.

6 EXPERIMENT RESULTS

A real-time implementation based on the feedforward FxLMS and 2GD-FxLMS algorithms in a NI PXIe 8880 controller was also carried out in a small noise chamber, as shown in Fig. 4. The audio amplifier TDA2030A

had a threshold of 750 mV. The NI PXIe-6368 module accomplished analog input, signal conditioning, and output of the system, with a sampling rate of 16 kHz. The length of the control filter and the secondary path estimate were chosen as 512 taps and 256 taps, respectively.

To understand the distortion created by the audio amplifier, we define the total harmonic distortion (THD) as

$$\mathrm{THD} = \frac{\sqrt{V_2^2 + V_3^2 + V_4^2 + \cdots}}{V_1} \tag{21}$$

where V_{n} $(n = 1, 2, \cdots)$ is root mean square (RMS) voltage of the nth harmonic and $n = 1$ is the fundamental frequency.

In the experiment, the two primary noise signals were tested: a 1 kHz tone, and a broadband signal from 500 Hz to 1.4 kHz. For the tonal noise, as shown in Fig. 5, FxLMS reduces the disturbance from 58 dB to 43 dB but cannot prevent the saturation distortion, resulting in a total harmonic distortion (THD) of 174%. In contrast, 2GD-FxLMS not only mitigate the disturbance to 53 dB but also prevents the audio amplifier from distortion with THD of 0.6%. For broadband noise, 2GD-FxLMS also suppresses the high-frequencies distortion better than FxLMS, as illustrated in Fig. 6.

7 CONCLUSION

This paper analyzed the amplitude and phase distortions created by the saturated audio amplifier and their effects on the performance of an ANC system. To deal with this issue, the previously proposed 2GD-FxLMS algorithm was applied. It has the same computational complexity as the conventional FxLMS and effectively suppresses the saturation distortion by restricting the output power of the audio amplifier. To validate the 2GD-FxLMS algorithm experimentally, it was implemented on an NI PXIe platform in a small noise chamber. The experiments verify that the algorithm can successfully mitigate the tonal and broadband noise, while preventing the audio amplifier from distortion. Further research could investigate the influence of the two step-sizes on the 2GD-FxLMS algorithm.

REFERENCES

[1] Kuo SM, Morgan D. Active noise control systems: algorithms and DSP implementations. John Wiley and Sons, Inc.; 1995 Jan 1.

[2] Chang, Cheng-Yuan, and Sheng-Ting Li. "Active noise control in headsets by using a low-cost microcontroller." IEEE Transactions on industrial electronics 58.5 (2011): 1936-1942.

[3] Kajikawa, Yoshinobu, Woon-Seng Gan, and Sen M. Kuo. "Recent advances on active noise control: open issues and innovative applications." APSIPA Transactions on Signal and Information Processing 1 (2012).

[4] Widrow, Bernard, John R. Glover, John M. McCool, John Kaunitz, Charles S. Williams, Robert H. Hearn, James R. Zeidler, JR Eugene Dong, and Robert C. Goodlin. "Adaptive noise cancelling: Principles and applications." Proceedings of the IEEE 63, no. 12 (1975): 1692-1716.

[5] Elliott, Stephen J., and Philip A. Nelson. "Active noise control." IEEE signal processing magazine 10.4 (1993): 12-35.

[6] Kuo, Sen M., and Dennis R. Morgan. "Active noise control: a tutorial review." Proceedings of the IEEE 87.6 (1999): 943-973.

[7] Shi C, Xie R, Jiang N, Li H, Kajikawa Y. Selective Virtual Sensing Technique for Multi-channel Feedforward Active Noise Control Systems. In ICASSP 2019-2019 IEEE International Conference on Acoustics, Speech and Signal Processing (ICASSP) 2019 Apr 17 (pp. 8489-8493). IEEE.

[8] Shi, Dong Yuan, Bhan Lam, and Woon-Seng Gan. "A Novel Selective Active Noise Control Algorithm to Overcome Practical Implementation Issue." 2018 IEEE International Conference on Acoustics, Speech and Signal Processing (ICASSP). IEEE, 2018.

[9] Bhan, Lam, and Gan Woon-Seng. "Active acoustic windows: Towards a quieter home." IEEE Potentials 35.1 (2016): 11-18.

[10] Shi, Dongyuan, Chuang Shi, and Woon-Seng Gan. "Effect of the audio amplifier's distortion on feedforward active noise control." 2017 Asia-Pacific Signal and Information Processing Association Annual Summit and Conference (APSIPA ASC). IEEE, 2017.

[11] George, Nithin V., and Ganapati Panda. "Advances in active noise control: A survey, with emphasis on recent nonlinear techniques." Signal processing 93.2 (2013): 363-377.

[12] Kajikawa, Yoshinobu. "The adaptive Volterra filter: Its present and future." Electronics and Communications in Japan (Part III: Fundamental Electronic Science) 83.12 (2000): 51-61.

[13] Patra, Jagdish Chandra, et al. "Identification of nonlinear dynamic systems using functional link artificial neural networks." IEEE transactions on systems, man, and cybernetics, part b (cybernetics) 29.2 (1999): 254-262.

[14] Liu, Chang, Zhi Zhang, and Xiao Tang. "Sign normalised spline adaptive filtering algorithms against impulsive noise." Signal Processing 148 (2018): 234-240.

[15] Costa, Márcio Holsbach, José Carlos M. Bermudez, and Neil J. Bershad. "Stochastic analysis of the LMS algorithm with a saturation nonlinearity following the adaptive filter output." IEEE transactions on signal processing 49.7 (2001): 1370-1387.

[16] Qiu, Xiaojun, and Colin H. Hansen. "A study of time-domain FXLMS algorithms with control output constraint." The Journal of the Acoustical Society of America 109.6 (2001): 2815-2823.

[17] Elliott, Stephen J., and K. H. Back. "Effort constraints in adaptive feedforward control." IEEE Signal Processing Letters 3.1 (1996): 7-9.

[18] Kozacky, Walter J., and Tokunbo Ogunfunmi. "Convergence analysis of an adaptive algorithm with output power constraints." IEEE Transactions on Circuits and Systems II: Express Briefs 61.5 (2014): 364-367.

[19] Zhang, Zhiyi, Fang Hu, and Junfang Wang. "On saturation suppression in adaptive vibration control." Journal of Sound and Vibration 329.9 (2010): 1209-1214.

[20] Lan, Hui, Ming Zhang, and Wee Ser. "A weight-constrained FxLMS algorithm for feedforward active noise control systems." IEEE Signal Processing Letters 9.1 (2002): 1-4.

[21] Tobias, Orlando José, and Rui Seara. "Leaky-FXLMS algorithm: stochastic analysis for Gaussian data and secondary path modeling error." IEEE Transactions on speech and audio processing 13.6 (2005): 1217-1230.

[22] Shi, DongYuan, et al. "Two-gradient direction FXLMS: An adaptive active noise control algorithm with output constraint." Mechanical Systems and Signal Processing 116 (2019): 651-667.

[23] Roberts, S. M., and H. I. Lyvers. "The gradient method in process control." Industrial and Engineering Chemistry 53.11 (1961): 877-882.

[24] Elliott, Stephen. Signal processing for active control. Elsevier, 2000.

[25] Hanson, Morgan A. "On sufficiency of the Kuhn-Tucker conditions." Journal of Mathematical Analysis and Applications 80.2 (1981): 545-550.